C. R. Physique 15 (2014) 448–457

Contents lists available at ScienceDirect

Comptes Rendus Physique

www.sciencedirect.com

Electromagnetism / Électromagnétisme

A quasi-universal method to measure the electromagnetic characteristics of usual materials in the microwave range

Méthode quasi universelle pour mesurer les caractéristiques électromagnétiques de tous types de matériaux dans le domaine des hyperfréquences

Élodie Georget *, Redha Abdeddaim, Pierre Sabouroux *

Aix–Marseille Université, CNRS, Centrale Marseille, Institut Fresnel, UMR 7249, Campus universitaire de Saint-Jérôme, avenue Escadrille-Normandie-Niemen, 13013 Marseille, France

ARTICLE INFO

Article history:
Available online 17 March 2014

Keywords:
Electromagnetic characterization
Relative permittivity
Sample holder
Coaxial cell
Flexible material

Mots-clés :
Caractérisation électromagnétique
Permittivité relative
Porte-échantillon
Cellule coaxiale
Matériau souple

ABSTRACT

Knowing the electromagnetic characteristics of different materials has become a major topic with the growing of wireless communications. The actual tools to perform this characterization have some limits, either in terms of limited frequency band, or in terms of inconstancy according to the different kinds of materials. On the basis of well-known procedures in the microwave domain, we present a new measurement cell equipped with a sample holder that can contain any kind of materials: solids, semi-solids (granular or powder materials), liquids. This technique can also characterize materials of thin thickness that are also more and more used in the RFID domain or in the realization of antennas on flexible substrates.

RÉSUMÉ

Aujourd'hui, connaître les valeurs expérimentales des caractéristiques électromagnétiques des différents matériaux devient incontournable avec l'avancée des communications sans fil. Les outils existants pour effectuer de telles caractérisations présentent des limites, soit en termes de bandes fréquentielles réduites, soit en termes de versatilité suivant les différents types de matériaux. Sur la base de procédures bien connues dans la communauté scientifique du domaine, nous présentons dans ce contexte une nouvelle cellule de mesure équipée d'un porte-échantillon pouvant confiner tous les types de matériaux : solides, semi-solides (matériaux granulaires ou pulvérulents), liquides. Cette technique permet aussi de caractériser des matériaux de faibles épaisseurs, qui sont aussi de plus en plus utilisés dans le domaine de la RFID ou des antennes sur substrats souples.

* Corresponding authors.

http://dx.doi.org/10.1016/j.crhy.2014.02.003
1631-0705/

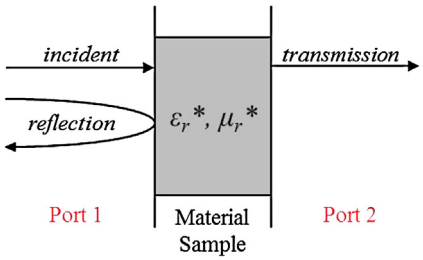

Fig. 1. Transmission/reflection configuration.

1. Introduction

Since 1946 [1], a dynamic in electromagnetic characterizations of materials has been set up. In the microwave range, several methods are used. They are based on reflection method [2], transmission method [3] or transmission/reflection method (Fig. 1) [4,5]. All these methods work in free space [6,7], coaxial line [8], waveguide [9], or resonant cavity [10]. Due to the multiplication of broadband communications, a new interest in broadband measurement appears. The above-mentioned methods have been readjusted for broadband measurement, either in processing with iterative methods of scattering parameters [11,12], or in the experimental part mixing several measurements [13,14].

The choice of the technique of measurement and the retrieving methods depends on the sample to characterize. In this paper, we present a single configuration to characterize different kinds of materials: solids, semi-solids (granule, powder, gel …) or liquids. This configuration is based on a coaxial line cell equipped with a containment area. The measurement of the scattering parameters of the cell is used to determine the relative permittivity $\epsilon_r = \epsilon' - j\epsilon''$ and permeability $\mu_r = \mu' - j\mu''$ via the modified Nicolson–Ross method.

Our methodology follows these different steps:

- The determination of the operating frequency band.
- The measurement of the experimental cell scattering S-parameters $[S_{cell}]$.
- The determination of the material sample scattering S-parameters $[S_{sample}]$ via a de-embedding step.
- The retrieving of the relative permittivity ϵ_r and permeability μ_r via the Nicolson–Ross procedure associated with a nonlinear algorithm.

After the presentation of our methodology, the results on different kind of materials (solid, granular, thin, liquid) are shown to validate our experimental setup.

2. Coaxial line cell with sample holder

All methods use only one mode in their frequency range. For a coaxial line, the fundamental mode is the Transverse ElectroMagnetic (TEM) mode. The cut-off frequency of the first higher order mode is $f_{c,TE_{11}}$ (Transverse Electric TE_{11} mode):

$$f_{c,TE_{11}} = \frac{c}{\pi (r_2 + r_1)\sqrt{\epsilon_r \mu_r}} \tag{1}$$

with c the speed of electromagnetic waves in vacuum, r_1 and r_2 the inner and outer radius of the coaxial line respectively, ϵ_r and μ_r the relative permittivity and permeability of the propagating medium, respectively. In Eq. (1), the cut-off frequency depends on the cell geometry, and on the relative permittivity ϵ_r and permeability μ_r of the material. In our case ($r_1 = 5.65/2$ mm, $r_2 = 13/2$ mm), the cut-off frequency of the empty cell is equal to 10 GHz.

In a coaxial configuration (Fig. 2a), several experimental uncertainties appear (Eq. (2)) [15]: measurement (magnitude and phase of the scattering parameters), line losses, connector mismatching, sample length (due to irregular sample surface, distances between the reference planes and the sample d_1 and d_2), air gaps between the sample and the coaxial line.

The uncertainties are described by the following equation [15]:

$$\frac{\Delta\gamma}{\gamma} = \frac{1}{\gamma} \times \sqrt{\delta} \tag{2}$$

with $\frac{\Delta\gamma}{\gamma}$ the uncertainty term of $\frac{\Delta\epsilon'}{\epsilon'}$ or $\frac{\Delta\epsilon'''}{\epsilon''}$. The term δ is equal to:

$$\delta = \sum_{\alpha}\left[\left(\frac{\partial\gamma}{\partial|S_\alpha|}\Delta|S_\alpha|\right)^2 + \left(\frac{\partial\gamma}{\partial\theta_\alpha}\Delta|\theta_\alpha|\right)^2\right] + \left(\frac{\partial\gamma}{\partial L}\Delta L\right)^2 + \left(\frac{\partial\gamma}{\partial d}\Delta d\right)^2 \tag{3}$$

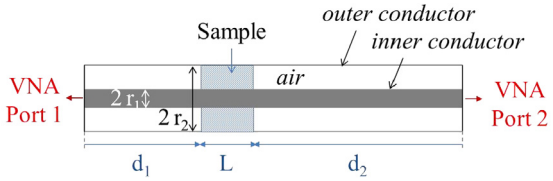

(a) Straight coaxial line configuration.

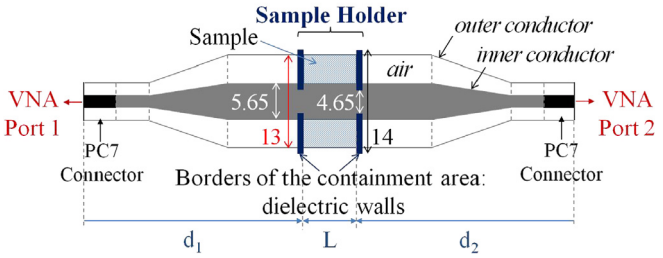

(b) Conical coaxial 13-mm cell configuration (all dimensions are in mm).

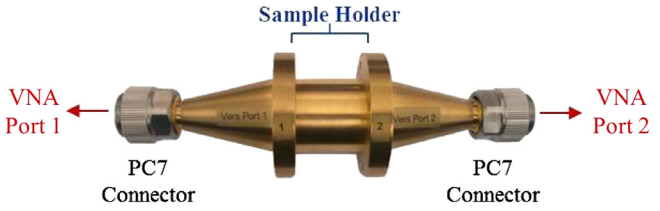

(c) Conical coaxial 13-mm cell realized.

Fig. 2. (Color online.) Different types of coaxial lines.

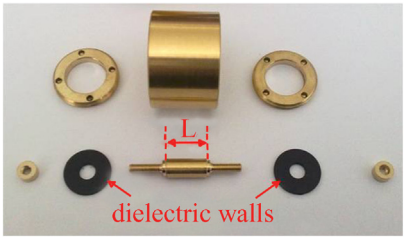

Fig. 3. (Color online.) Dismantled sample holder.

The measurement uncertainty (first term in Eq. (3)) is the sum of the S_{11} parameter uncertainty and the S_{21} parameter uncertainty ($\alpha = 11$ or 21 in Eq. (3)), each parameter uncertainty being decomposed in magnitude uncertainty $\Delta|S_\alpha|$ and in phase uncertainty $\Delta\theta_\alpha$. The last two terms represent the material sample uncertainties, on the sample length ΔL and on the air gap Δd (with d the air gap distance between the sample and the coaxial conductors).

To reduce the material sample uncertainties, we design a new measurement cell (Figs. 2b and 2c). The originality of this cell is its segmentation in three parts: the central containment area of material sample, the transition lines, and the connectors. The connectors are Precision Connectors of 7 mm outer diameter (PC7). The outer diameter of the containment area is chosen equal to 13 mm to have a larger volume than the work area of the straight coaxial line of outer diameter 7 mm for a sample of the same length L. To realize the transition lines between the work area and the connectors, the conical geometry is designed.

The containment area is delimited by two dielectric walls (Fig. 3). Thanks to this containment area, the sample holder is able to contain a material sample whatever its state: solid, liquid, powder, granular … The length L of the material sample is not fixed: two lengths of the sample holder are used in this study (3 mm and 12 mm).

This containment area permits to minimize the uncertainties. Indeed, the air-gap distance d, the length sample L and the distances d_1 and d_2 are better known. The Δd and ΔL uncertainties are minimized in Eq. (3).

The cell exhibits a characteristic impedance of $Z_c = 50\ \Omega$ in the straight and conical parts respecting Eq. (4) [16] with $\epsilon_{r,air} = 1$.

$$Z_c = \frac{60}{\sqrt{\epsilon_r}} \times \ln\left(\frac{r_2}{r_1}\right) \tag{4}$$

The addition of two walls in the containment area adds a slight mismatching of impedance. They have slightly less than a 50-Ω characteristic impedance (45.6 Ω for Teflon walls), but this will be taken into account in the next part of this paper (Section 3.1).

3. Processing of measurements

After the description of the cell, the different steps of measurement processing are presented.

3.1. De-embedding operation

We need to know the scattering matrix of the material sample $[S_{sample}]$. This is recovered from the cell matrix $[S_{cell}]$ by a de-embedding step. This method is expressed in Eqs. (5)–(8).

$$S_{sample,11} = S_{cell,11} \times \exp\big(jk(2d_1)\big) \times \exp\big(\alpha(2d_1)\big) \tag{5}$$

$$S_{sample,21} = S_{cell,21} \times \exp\big(jk(d_1 + d_2)\big) \times \exp\big(\alpha(d_1 + d_2)\big) \tag{6}$$

$$S_{sample,12} = S_{cell,12} \times \exp\big(jk(d_1 + d_2)\big) \times \exp\big(\alpha(d_1 + d_2)\big) \tag{7}$$

$$S_{sample,22} = S_{cell,22} \times \exp\big(jk(2d_2)\big) \times \exp\big(\alpha(2d_2)\big) \tag{8}$$

with $k = \frac{2\pi}{\lambda_0}$ the wavenumber in vacuum, d_1 and d_2 the electrical distances, and α the attenuation coefficient of the coaxial line.

In these equations, two exponential terms are discerned, the phase propagation term exp($jk \times$ distance) generally used [15] and the line attenuation propagation term exp($\alpha \times$ distance).

The attenuation of a straight coaxial line is given by the conductor attenuation α_c and the dielectric attenuation α_d [17]:

$$\begin{aligned}\alpha &= \alpha_c + \alpha_d \\ &= \frac{1}{2}\sqrt{\frac{\epsilon_0\epsilon_r f\pi}{\sigma}}\left(\frac{1}{r_2} + \frac{1}{r_1}\right)\left(\frac{1}{\ln(r_2/r_1)}\right) + \pi f \tan(\delta)\sqrt{\epsilon_0\epsilon_r\mu_0\mu_r} \quad (\text{Np/m})\end{aligned} \tag{9}$$

where μ_r, ϵ_r and $\tan(\delta)$ are the relative permeability and the relative permittivity and the loss tangent of the medium, respectively. For the cell without the material sample, $\mu_r = 1$, $\epsilon_r = 1$ and $\tan(\delta) = 0$. The permeability of the vacuum is $\mu_0 = 4\pi \times 10^{-7}$ H/m, the permittivity of the vacuum is $\epsilon_0 = \frac{1}{36\pi} \times 10^{-9}$ F/m, and σ is the conductivity of the inner and outer conductors. This expression α in Eq. (9) does not take into account the geometry of the conical coaxial line. For more precision, the attenuation of the 13-mm cell is determined from the S_{21} measurement of the empty cell:

$$|S_{\text{empty cell},21}| = \big|\exp\big(-jk(d_1 + L + d_2)\big)\big| \times \big|\exp\big(-\alpha(d_1 + L + d_2)\big)\big| \tag{10}$$

$$\alpha = -\frac{\ln(|S_{\text{empty cell},21}|)}{d_1 + L + d_2} \tag{11}$$

In our case, the $S_{\text{empty cell},21}$ is the measurement of the S_{21} parameter of the empty cell with the two dielectric walls in order to take them into account in the processing. The distances d_1 and d_2 were previously measured inserting a short circuit in the sample holder. With the measured attenuation cell α, and the measured distances d_1 and d_2, the conical geometry cell, the dielectric walls and the connectors mismatching are taken into account. After the de-embedding processing, the $[S_{sample}]$ matrix is obtained.

3.2. Electromagnetic parameters of the sample

The S-parameters of the material sample $[S_{sample}]$ are now retrieved and the Nicolson–Ross method can be applied to this matrix. The sample scattering coefficients S_{11} and S_{21} are linked to the reflection Γ and transmission T coefficients by Eqs. (12) and (13):

$$\Gamma = \frac{1 + S_{11}^2 - S_{21}^2}{2S_{11}} \pm \sqrt{\left(\frac{1 + S_{11}^2 - S_{21}^2}{2S_{11}}\right)^2 - 1} \tag{12}$$

$$T = \frac{S_{11} + S_{21} - \Gamma}{1 - (S_{11} + S_{21})\Gamma} \tag{13}$$

$$z_r = \sqrt{\mu_r/\epsilon_r} = \left(\frac{1+\Gamma}{1-\Gamma}\right) \tag{14}$$

To respect physical solutions, the magnitude of the reflection coefficient must be $|\Gamma| \leqslant 1$, and the real part of the reduced impedance z_r (Eq. (14)) must be positive $\Re(z_r) > 0$.

The relative permittivity ϵ_r and permeability μ_r are given by:

$$\mu_r = \mathrm{j}\frac{c}{2\pi f L}\left(\frac{1+\Gamma}{1-\Gamma}\right)\ln(1/T) \tag{15}$$

$$\epsilon_r = \mathrm{j}\frac{c}{2\pi f L}\left(\frac{1+\Gamma}{1-\Gamma}\right)^{-1}\ln(1/T) \tag{16}$$

Due to the logarithm operator in Eqs. (15) and (16), the relative permittivity ϵ_r and permeability μ_r have an infinite number of solutions. The problem can be solved by the group-delay method [5] or the phase unwrapping method. It is possible to decompose this problem into two parts: determination of the initial phase, and phase unwrapping. The new expressions of the relative permeability μ_r and permittivity ϵ_r are:

$$\mu_r = \mathrm{j}\frac{c}{2\pi f L}\left(\frac{1+\Gamma}{1-\Gamma}\right)\left[-\ln(T) - \left(\mathrm{j}\theta(T) + 2\pi n\right)\right] \tag{17}$$

$$\epsilon_r = \mathrm{j}\frac{c}{2\pi f L}\left(\frac{1+\Gamma}{1-\Gamma}\right)^{-1}\left[-\ln(T) - \left(\mathrm{j}\theta(T) + 2\pi n\right)\right] \tag{18}$$

To correct the phase jumps of the transmission T coefficient knowing the initial value, an unwrapping processing step is applied. The number and the position of the phase jumps allow evaluating the initial value of this phase. This step is possible because this method works on broadband frequency in a coaxial configuration.

After this step, these results can be linearized with a nonlinear least-square method.

3.3. Nonlinear least-square method

For low-loss materials at frequencies corresponding to integer multiples of one-half wavelength in the sample $\lambda_s/2$, some large variations of the relative permittivity and permeability results exist. The relation between the resonant wavelength in the sample λ_s and the length of the resonator sample L is:

$$L = n\frac{\lambda_s}{2} \tag{19}$$

with n corresponding to an integer $n = 1, 2, 3, \ldots$ and $\lambda_s = \frac{\lambda_0}{\sqrt{\epsilon_r \mu_r}}$ (λ_0 corresponding to the wavelength in vacuum). Results diverge at frequencies:

$$f_n = n\frac{c}{2L\sqrt{\epsilon_r \mu_r}} \tag{20}$$

To eliminate these discrepancies, a solution is based on a nonlinear process minimizing the square error [18]. This method is suitable for obtaining complex permittivity and permeability spectra of isotropic, homogeneous materials. A frequency-dependent form for ϵ_r and μ_r is used for the determination of ϵ_r and μ_r. According to the Debye model, the permittivity of a material can be expressed in the form:

$$\epsilon_r = \frac{1}{1 + \mathrm{j}B(2\pi f)} + C \tag{21}$$

where B and C are constants and f is the frequency. On this basis, we can assume a series of poles of the first order for ϵ_r and μ_r:

$$\mu_r(f) = A_0 + \sum_i \frac{A_i}{1 + \mathrm{j}B_i(2\pi f)} \tag{22}$$

$$\epsilon_r(f) = C_0 + \sum_i \frac{C_i}{1 + \mathrm{j}D_i(2\pi f)} \tag{23}$$

Excellent results are obtained with the above expressions, where B_i and D_i are real numbers. The poles should all reside in the left half plane. The constants are initialized to the value of the relative permittivity and permeability calculated by the Nicolson–Ross method at a fixed frequency, 1 GHz in this paper: $A_0 = \epsilon_{r,\mathrm{NR}}(1\ \mathrm{GHz})$ and $C_0 = \mu_{r,\mathrm{NR}}(1\ \mathrm{GHz})$. The method to determine B_i, C_0, C_i, D_i consists in minimizing the sum of the differences between the predicted P and measured S-parameters:

$$\min\left\|\sum_{ij}(S_{ij}-P_{ij})\right\| \tag{24}$$

where the X-parameter ($X = P$ or S) vector is expressed as $X_{ij} = (X_{ij}(f_1), X_{ij}(f_2), \ldots, X_{ij}(f_n))$ with $ij = 11$ or 21.

In order to obtain good values of the relative permittivity and permeability, the Nicolson–Ross method must be completed by an unwrapping step and a linearization step using the nonlinear least-square method.

4. Results and validation

To validate this technique, it was tested on samples of different physical natures: solids, semi-solids, and liquids. For each kind of materials, the Nicolson–Ross method (NR) associated with an unwrapping processing step is applied and completed by the Nonlinear Least SQuare method (NLSQ). The studied frequency band is between 100 MHz and 10 GHz.

4.1. Example of solid material: high-density polyethylene

For solids, the technique is tested on a very classical material, High-Density PolyEthylene [19]. This material was tested, on the one hand, with the 13-mm cell and, on the other hand, with a reference cell: a straight coaxial line (air line 7 mm [20]) (Fig. 4a). The results obtained using the two different cells are displayed in Fig. 5.

The results obtained with the 13-mm conical cell and the ones obtained with the straight 7-mm coaxial cell are in a good agreement. The differences between the results of the NSLQ method and those of the NR method before 500 MHz show the limit of the linearization of the NLSQ method at low frequencies. The variations of the results obtained with the NR method after 7 GHz are due to the arrival of the higher-order mode in the material. This is valid for all materials.

(a) 7-mm cell for solid material measurements.

(b) 13-mm cell for solid, semi-solid, fine materials measurements.

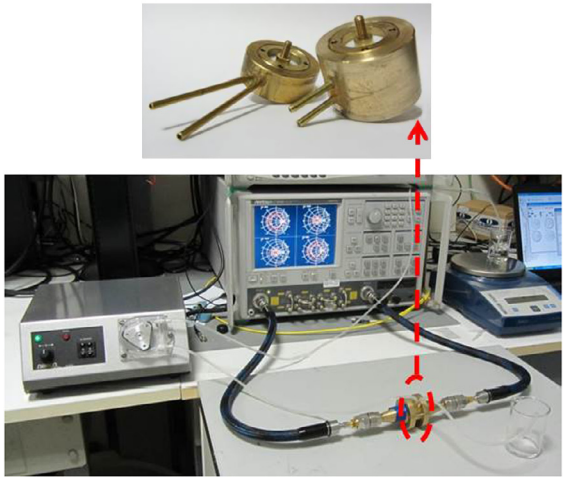

(c) Configuration for liquid measurement (sample holder at the top, experimental cell with pump system at the bottom).

Fig. 4. (Color online.) Setup measurements for different kinds of materials.

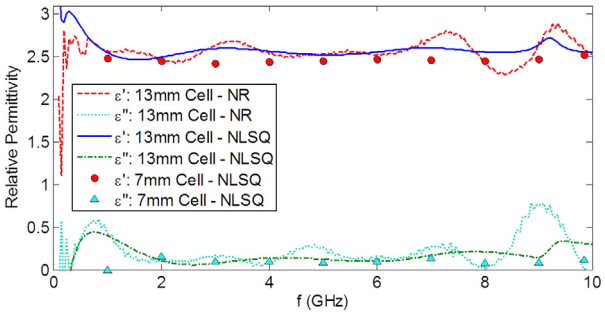

Fig. 5. (Color online.) Relative permittivity of HDPE.

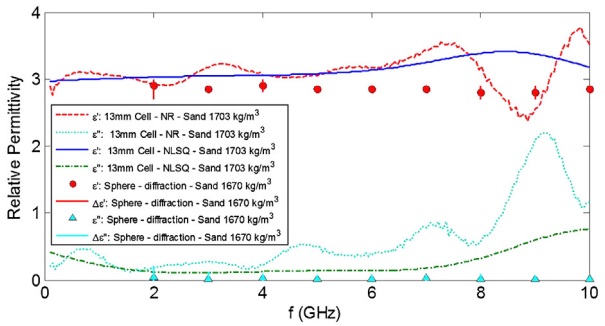

Fig. 6. (Color online.) Relative permittivity of sand.

Fig. 7. (Color online.) Flexible samples.

4.2. Example of granular material: sand

For semi-solids, the technique was validated on sand samples from the Dune of Pilat in France [21] sifted to get a size grading between 200 and 300 µm. The results have been compared to some results obtained from scattered field measurements in free space of a PMMA (PolyMethyl MethAcrylate, i.e. Plexiglas) sphere filled with this same sand. These values of permittivity have been obtained minimizing a criterion of comparison between measurements and results of modeling from a Mie analytical model [22].

The results of permittivity with the scattered field measurements (Fig. 6) are slightly lower than the results with our experimental cell, because the density of the sand in the sphere is a little bit lower than the density of the sand in the sample holder. The results of the two methods on our sample under test and those of the other method of scattered fields are in a good agreement.

4.3. Example of thin material: flexible substrate

The thin samples were inserted in the sample holder by making a pile of disks of flexible substrate (Fig. 7). The results obtained with the two processing method for the relative permittivity are consistent (Fig. 8); the NSLQ method linearizes the results of the NR method.

However, because no result is available in the literature for these particular textile materials, the only option to validate these values is to simulate a radiating element using this coating cloth as a substrate. A monopole antenna printed on this flexible substrate is simulated with the CST Microwave Studio software, taking into account the values of permittivity previously measured. Then, a prototype of this antenna was realized and measured in term of adaptation (Fig. 9).

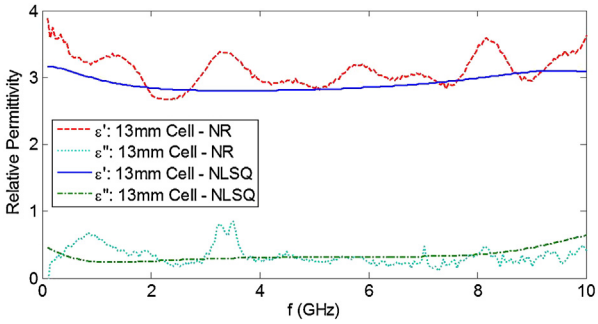

Fig. 8. (Color online.) Relative permittivity of flexible substrate.

(a) Antenna.

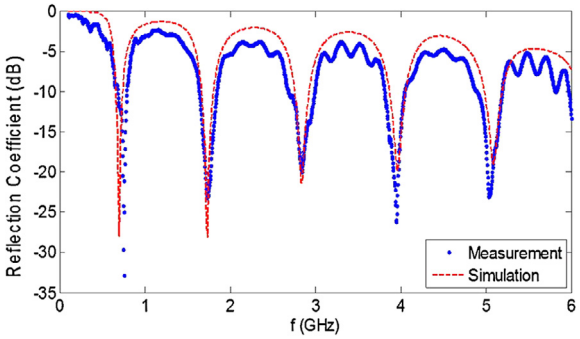

(b) Reflection coefficient of the antenna.

Fig. 9. (Color online.) Monopole test antenna on flexible substrate of permittivity $\epsilon_r^* = (3.0 - j0.4)$.

We observe that the resonance frequencies in simulation and in measurements in Fig. 9b are in good agreement, with a frequency shift always less than 60 MHz, which is less than 8% at these frequencies. The determination of the relative permittivity of flexible materials is validated.

4.4. Example of liquid material: ethanol

For the liquid materials, the sample holder has been adapted with microtubes to fill the containment area with a liquid (Fig. 4c). The results obtained with ethanol have been compared with results from the literature [23,24].

Liquid ethanol is injected into a sample holder of 12 mm length (net volume: 1.3 cm^3). The liquid was inserted in the sample holder using a pump to make sure this filling. The results have been compared to values from the literature [24] obtained via another technique, the open-ended coaxial line (Fig. 10). This technique is usually used for the electromagnetic characterization of liquid materials. The NLSQ method is not used here, since the variations of permittivity characterize the material.

The results with the experimental cell and with the open-ended coaxial line are in a good agreement, in spite of a slight difference.

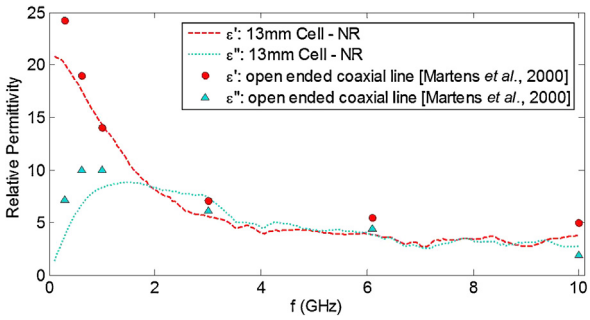

Fig. 10. (Color online.) Relative permittivity of ethanol.

5. Conclusion

The conical transmission cell with the sample holder presented here is suitable for electromagnetic measurement in terms of relative permittivity ϵ_r and permeability μ_r. The advantage of this cell is that the sample holder can contain different kinds of materials: solid, granular, thin, and liquid. The experimentations have been validated between 100 MHz and 10 GHz on each kind of material by comparing to literature values or to known applications. The nonlinear least-square algorithm permits to correct the discrepancies.

The sample holder in the cell can be designed with different lengths L. Up to now, sample holders of lengths 3, 6, 12, and 24 mm have been realized. The independent sample holder of the cell enables to prepare a sample in an independent way of the microwave measurement. This is important if the place of preparation of the sample to test is different from the place of the measurement. For example, if the material to test is a biological liquid requiring a sterile environment, in these conditions, the sample holder can be sterilized on the one hand, and the sample can be positioned in the sample holder in a sterile enclosure on the other hand. Then, the person who prepares the sample is not necessarily the same person as the one who carries out the microwave measurement.

Acknowledgements

We thank Thomas Lepetit for his collaboration in the nonlinear square algorithm. We also thank Christelle Eyraud and Jean-Michel Geffrin who have realized the scattered field method of the sand.

References

[1] S. Roberts, A. Von Hippel, A new method for measuring dielectric constants and loss in the range of centimeter waves, J. Appl. Phys. 7 (1946) 610–616.
[2] M.A. Stuchly, S.S. Stuchly, Coaxial line reflection methods for measuring dielectric properties of biological substances at radio and microwave frequencies—a review, IEEE Trans. Microw. Theory Tech. 29 (1980) 176–183.
[3] A.H. Muqaibel, A. Safaai-Jazi, A new formulation for characterization of materials based on measured insertion transfer function, IEEE Trans. Microw. Theory Tech. 51 (2003) 1946–1951.
[4] A.M. Nicolson, G.F. Ross, Measurement of the intrinsic properties of materials by time-domain techniques, IEEE Trans. Instrum. Meas. 19 (1970) 377–382.
[5] W.B. Weir, Automatic measurement of complex dielectric constant and permeability at microwave frequencies, Proc. IEEE 62 (1974) 33–36.
[6] D.K. Ghodgaonkar, V.V. Varadan, V.K. Varadan, A free-space method for measurement of dielectric constants and loss tangents at microwave frequencies, IEEE Trans. Instrum. Meas. 38 (1989) 789–793.
[7] Z. Awang, et al., A free-space method for complex permittivity measurement of bulk and thin film dielectrics at microwave frequencies, PIER B 51 (2013) 307–328.
[8] M. Adous, P. Quéffélec, L. Laguerre, Coaxial/cylindrical transition line for broadband permittivity measurement of civil engineering materials, Meas. Sci. Technol. 17 (8) (2006) 2241–2246.
[9] O. Ogunlade, R.D. Pollard, I.C. Hunter, A new method of obtaining the permittivity of liquids using in-waveguide technique, IEEE Microw. Wirel. Compon. Lett. 16 (2006) 363–365.
[10] L. Li, et al., Evaluation of microwave dielectric properties of giant permittivity materials by a modified resonant cavity method, Appl. Phys. Lett. 91 (2006), 092906-1–092906-3.
[11] J. Baker-Jarvis, E.J. Vanzura, W.A. Kissick, Improved technique for determining complex permittivity with the transmission/reflection method, IEEE Microw. Instrum. Meas. 38 (1990) 1096–1103.
[12] U.C. Hasar, A new microwave method based on transmission scattering parameter measurements for simultaneous broadband and stable permittivity and permeability determination, PIER 93 (2009) 161–176.
[13] U.C. Hasar, et al., Resolving phase ambiguity in the inverse problem of reflection-only measurement methods, PIER 129 (2012) 405–420.
[14] J.M. Catalá-Civera, et al., A simple procedure to determine the complex permittivity of materials without ambiguity from reflection measurements, MOLT 25 (2000) 191–194.
[15] J. Baker-Jarvis, et al., Transmission/reflection and short-circuit line methods for measuring permittivity and permeability, Technical Report, NIST, 1993.
[16] L.F. Chen, et al., Microwave Electronics: Measurement and Materials Characterization, Wiley, Chichester, UK, 2004.
[17] P.F. Combes, Micro-ondes. Tome 1. Lignes, guides et cavités, Dunod, Paris, 1996.
[18] J. Baker-Jarvis, R.G. Geyer, P.D. Domich, A nonlinear least-squares solution with causality constraints applied to transmission line permittivity and permeability determination, IEEE Microw. Instrum. Meas. 41 (1992) 646–652.

[19] B. Riddle, J. Baker-Jarvis, J. Krupka, Complex permittivity measurements of common plastics over variable temperatures, IEEE Trans. Microw. Theory Tech. 51 (2003) 727–733.
[20] P. Sabouroux, www.epsimu.fr, 2008–2014.
[21] D. Ba, P. Sabouroux, EpsiMu, a toolkit for permittivity and permeability measurement in microwave domain at real time of all materials: applications to solid and semisolid materials, MOTL 52 (2010) 2643–2648.
[22] H. Tortel, Localization and derivation of an optimal sphere for 3d perfectly conducting objects, J. Electromagn. Waves Appl. 16 (2002) 771–791.
[23] P. Petong, P. Pottel, U. Kattze, Water–ethanol mixtures at different compositions and temperatures. a dielectric relaxation study, J. Phys. Chem. 104 (2000) 7420–7428.
[24] H.C.F. Martens, J.A. Reedijk, H.B. Brom, Measurement of the complex dielectric constant down to helium temperatures. i. Reflection method from 1 MHz to 20 GHz using an open ended coaxial line, Rev. Sci. Instrum. 71 (2000) 473–477.